ACS APPLIED MATERIALS & INTERFACES
Research Article
www.acsami.org

In/Ga-Free, Inkjet-Printed Charge Transfer Doping for Solution-Processed ZnO

Seong Hun Yu,[†] Beom Joon Kim,[‡] Moon Sung Kang,[§] Se Hyun Kim,[∥] Jong Hun Han,[⊥] Jun Young Lee,*[,†] and Jeong Ho Cho*[,†,‡]

[†]School of Chemical Engineering, Sungkyunkwan University, Suwon, 440-746, Korea

[‡]SKKU Advanced Institute of Nanotechnology (SAINT) and Center for Human Interface Nano Technology (HINT), Sungkyunkwan University, Suwon, 440-746, Korea

[§]Department of Chemical Engineering, Soongsil University, Seoul, 156-743, Korea

[∥]Department of Advanced Organic Materials Engineering, Yeungnam University, Gyeongsan, 712-749, Korea

[⊥]Department of Applied Chemical Engineering, Chonnam National University, Gwangju 500-757, Korea

S *Supporting Information*

ABSTRACT: An In/Ga-free doping method of zinc oxide (ZnO) is demonstrated utilizing a printable charge transfer doping layer (CTDL) based on (3-aminopropyl)-triethoxysilane (APS) molecules. The self-assembled APS molecules placed on top of ZnO thin films lead to *n*-type doping of ZnO and filling shallow electron traps, due to the strong electron-donating characteristics of the amine group in APS molecules. The CTDL doping can tune the threshold voltage and the mobility of the ZnO thin-film transistors (TFTs) as one varies the grafting density of the APS molecules and the thickness of the underneath ZnO thin films. From an optimized condition, high-performance ZnO TFTs can be achieved that exhibit an electron mobility of 4.2 $cm^2/(V\ s)$, a threshold voltage of 10.5 V, and an on/off current ratio larger than 10^7. More importantly, the method is applicable to simple inkjet processes, which lead to produce high-performance depletion load ZnO inverters through selective deposition of CTDL on ZnO thin films.

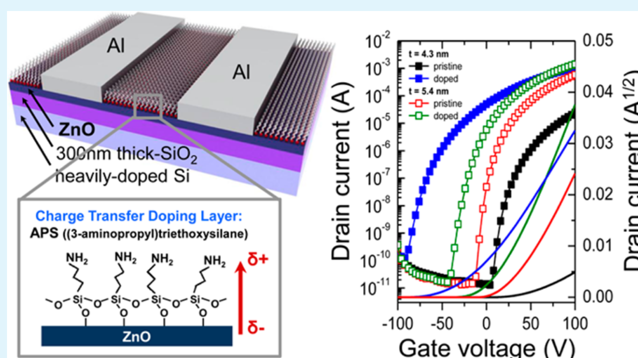

KEYWORDS: *charge transfer doping layer, solution-processed zinc oxide, carrier mobility, thin-film transistor, depletion load inverter*

1. INTRODUCTION

Demands for high-performance, large-area, and low-cost electronic devices have led a boost in development of alternative semiconducting materials to traditional silicon.[1−5] Solution-processed zinc oxides (ZnO), in particular, are very attractive semiconductors for implementation into thin-film transistors (TFTs). This is mainly because ZnO exhibits high electron mobility, environmental stability, optical transparency, and solution-processability.[6−14] To further enhance their electrical properties, doping—a process of introducing electronic impurities into semiconductors—of ZnO has attracted signficant research interest recently.[15−17] Successful doping of ZnO would provide means (i) to further enhance electron mobility necessary for display technologies and (ii) to control threshold voltage in TFTs useful for logic circuit designing.[10,15,18−22] Traditionally, ZnO doping has been carried out employing the group IIIA elements, such as In or Ga.[23−29] The resulting doped ZnO materials are more often called as IZO (indium-doped zinc oxide) or IGZO (indium gallium zinc oxide). Despite the improved electrical properties of these doped ZnO semiconductors, however, there remain critical issues for utilizing IZO or IGZO in electronic devices. Because of the supply shortage of indium, the cost of indium has increased rapidly, and in fact, indium has even become one of the strategic materials. Therefore, developing alternative low-cost and simple doping methods is critical for practical applications of solution-processed ZnO TFTs.

To address this issue, we introduce a charge transfer doping layer (CTDL) onto ZnO TFTs via solution processes, such as drop-casting and inkjet printing. Doping was controlled upon tuning the underneath ZnO layer thickness and/or the grafting density of CTDL on the ZnO systematically. Doping turned out to be more effective on a thinner ZnO layer with higher grafting density. The optimized devices yield an enhanced electron mobility around 4.2 $cm^2/(V\ s)$ with more than 7 orders of magnitude in current modulation. Furthermore, the capability of simple threshold voltage control was applied to demonstrate high-performance depletion load ZnO inverters

Received: July 19, 2013
Accepted: September 13, 2013
Published: September 13, 2013

ACS Publications © 2013 American Chemical Society

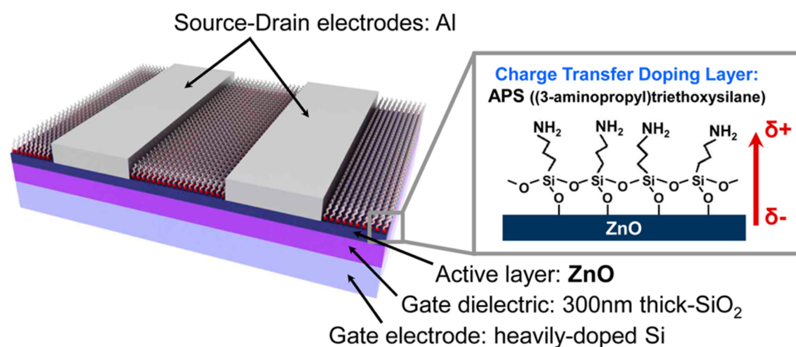

Figure 1. Schematic diagram of the charge transfer doping layer (CTDL)-doped ZnO TFTs. The inset describes the formation of dipole in CDTL.

based on selective deposition of CTDL by inkjet printing. We believe that the method presented in this report can provide new directions in low-cost, high-performance, solution-processed ZnO TFT research.

2. EXPERIMENTAL SECTION

A ZnO solution was prepared by dissolving 0.6, 0.7, 0.8, 0.9, and 1 mmol of zinc oxide powder (Sigma Aldrich, 99.999%) into 12 ml of ammonium hydroxide (aq). The as-prepared solution was refrigerated for more than 12 h. Refrigeration enhanced the solubility of ZnO and resulted in an optically clear solution of ZnO. This ZnO solution was spin-coated onto a UV−ozone treated SiO_2/Si substrate for 30 s at 3000 rpm, follwed by an annealing process at 300 °C for 1 h. After depositing ZnO film, 50 nm thick Al source/drain electrodes were thermally deposited through a shadow mask. The channel length (L) and width (W) were 50 and 800 μm, respectively. Finally, the ZnO surface was treated with 0.085 mM (3-aminopropyl)triethoxysilane (APS) solution in toluene by immersing the substrate with ZnO films into the APS solution for different periods of time (0, 1, 2 ,4, 8 h). For the fabrication of the depletion load inverters, two ZnO transistors were prepared for the load and driver transistors, respectively. The source and gate electrodes of the load transistor were connected together, and then the drain electrode of the drive transistor was connected to the source electrode of the load transistor using silver paste. A single droplet of 0.02 mM CTDL solution in chloroform was printed onto the ZnO channel surface of the load transistor using a home-built inkjet printer. Transistor and inverter current−voltage characteristics were measured using Keithley 2400 and 236 source/measure units under vacuum (10^{-5} Torr) in a dark environment. Threshold voltage (V_{th}) and electron mobility (μ) in the saturation region were evaluated from the x intercept and slope of the transfer curve (drain current $(I_D)^{1/2}$ vs gate voltage (V_G)), respectively, using the following equation

$$I_D = \frac{\mu C_i}{2}\frac{W}{L}(V_{GS} - V_{th})^2$$

where L and W are the length and width of the channel and C_i is the specific capacitance of gate dielectric. The thickness of ZnO film was measured by X-ray reflectivity and ellipsometry. Film morphology and chemical composition of the doped/undoped ZnO films were investigated by AFM (Digital Instruments Nanoscope III) and XPS (PHI 5000 VersaProbe ll, ULVAC-PHI 5000 VersaProbe), respectively.

3. RESULTS AND DISCUSSION

A schematic of a ZnO TFT with CTDL in a bottom gate, top contact configuration is drawin in Figure 1, which was prepared by the following procedures. First, ZnO thin films were formed by spin-coating a dispersion of zinc oxide powder in ammmonium hydroxide onto a heavily doped Si substrate with a 300 nm thick SiO_2 gate dielectric. The substrate was then annealed at 300 °C under an ambient condition for 1 h, which transformed the zinc ammonia complex into ZnO films and volatile ammonia gas.[15] ZnO films with various thicknesses (4.3, 4.7, 5.4, 6.5, and 7.2 nm) could be obtained from disperpersions with different concentrations (4.1, 4.8, 5.4, 6.1, and 6.8 mg/mL, respectively). To generate hydroxyl groups on the ZnO surface, the as-prepared films were treated to UV−ozone (28 mW/cm^2, 30 s). The CTDL of (3-aminopropyl)-triethoxysilane (APS) was then applied onto the surface through a simple dipping method. Upon exposure to APS solution, the CTDL was self-assembled onto ZnO films through hydrolysis of the triethoxy groups of APS and condensation of the hydroxyl groups in APS and the ZnO surface, as shown in Figure 1.[30] Grafting of the APS onto ZnO films could be controlled by varying the reaction time for self-assembly (1, 2, 4, and 8 h). The variation in the grafting density was confimed by X-ray photoemission spectroscopy (XPS) as a function of treatment time (Figure S1, Supporting Information): longer exposure to the APS solution resulted in formation of denser CTDL exhibiting a higher N-to-Zn atomic ratio. Also, increasing the APS exposure time yielded a gradual enhancement of film roughness, indicating formation of denser CTDL (Figure S2, Supporting Information), whereas no significant change was observed upon varying the ZnO film thickness (Figure S3, Supporting Information). Finally, Al was thermally evaporated through a stencil mask onto the doped ZnO film to form the source/drain electrodes.

Figure 2a displays the representative transfer characteristics of TFTs based on 4.3 and 5.4 nm thick ZnO films before and after introducing the CTDL for 1 h. Dramatic reduction in the V_{th} was noticed, which is a key signature of n-type doping that resulted from the charge transfer doping.[15] The charge transfer doping orginates from the electron-donating nature of amine

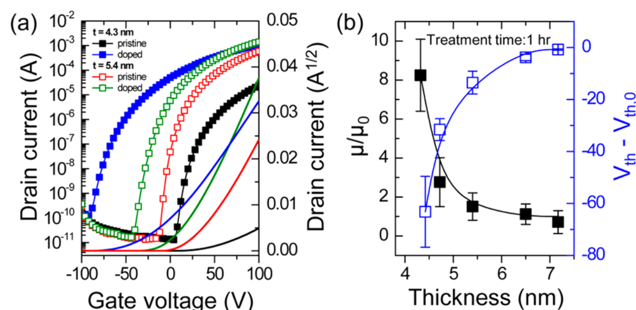

Figure 2. (a) Transfer characteristics (V_D = 60 V) of ZnO TFTs based on 4.3 and 5.4 nm thick ZnO films before and after the CTDL treatment. (b) μ/μ_0 vs thickness and the $V_{th} - V_{th,0}$ vs thickness plots after CTDL treatment for 1 h as a function of the ZnO thickness.

group in the APS molecules. This leads to formation of a dipole that facilitates inducing mobile electrons in ZnO (see the inset in Figure 1). V_{th} shifts (ΔV_{th}'s) were −63 and −14 V for ZnO TFTs based on the 4.3 and 5.4 nm thick ZnO films, respectively. More importantly, the charge transfer doping yielded a drastic enhancement in the μ from 0.1 to 0.8 cm^2/(V s) for the 4.3 nm thick ZnO TFT and from 1.4 to 2.0 cm^2/(V s) for the 5.4 nm thick ZnO TFT.

The effectiveness of charge transfer doping was quantified by comparing the mobility enhancement and the threshold voltage shift for ZnO films with different thicknesses. Figure 2b displays the μ/μ_0 (μ_0 is the mobility of the pristine ZnO films at a given thickness) and $V_{th} - V_{th,0}$ ($V_{th,0}$ is the threshold voltage of the pristine ZnO films at a given thickness) obtained from samples with different thicknesses. The representative transfer characterstics and summarized electrical parameters are shown in Figure S4 and Table S1 (Supporting Information). Clearly, the effectiveness of the charge transfer doping is suppressed gradually as the film becomes thicker: both the slopes from the μ/μ_0 vs thickness and the $V_{th} - V_{th,0}$ vs thickness plots become saturated above 6.5 nm. This is perhaps because the effective charge tranport channel in a bottom-gated TFT is located at the very bottom layer of the semiconductor adjacent to the gate dielectric layer, while the charge transfer doping occurs from the top layer of the semiconductor.[31] In other words, if the semiconductor is too thick, carriers from the CTDL may not affect the charge transport in the effective channel. In fact, the effective channel thickness is estimated to be <1 nm at a V_G of 100 V, using an equation developed for enhancement-mode organic TFTs.[32,33] Figure S5 (Supporting Information) compares the output characteristics for the 4.3 and 5.4 nm thick ZnO TFTs before and after applying CTDL, indicating that more effective doping is achievable on thinner ZnO TFTs.

The charge transfer doping could also be controlled by varying the treatment time. Figure 3a shows the change of the transfer characteristics of 5.4 nm thick ZnO TFTs that were dipped into APS solution for different periods of time (0, 1, 2, 4, and 8 h). A gradual increase in I_D and a negative shift in V_{th} were observed upon increasing the reaction time as a result of enhanced charge tranfer doping. The effects of the APS reaction time on the μ and V_{th} are summarized in Figure 3b and Table S2 (Supporting Information). The ZnO TFTs that were treated with APS for 4 h yielded excellent device performance with an electron mobility of 4.2 cm^2/(V s) and an on/off current ratio of more than 10^7. Note that an excess adsorption of APS (when APS was applied for more than 8 h) produced heavily doped ZnO films such that mobility as high as 6.3 cm^2/(V s) could be obtained. However, these devices unfortunately exhibited a weak gate voltage dependence in the transfer characteristics due to excess doping.

On the basis of the V_{th} shift compared to the pristine device, the effective doping density of the CTDL (n_{doping}) could be estimated using a relation $n_{doping} = C\Delta V_{th}/e$, where C is the specific capacitance of the gate dielectric (10.8 nF/cm^2) and e is the elementary charge. A doping density of $\sim 10^{12}$ electrons/cm^2 could be achieved, which increased gradually with APS reaction time. Figure 3c correlates the estimated n_{doping} values with electron mobility, which demonstrates the enhanced electron mobility in ZnO films with increased charge density.

An increase of mobility with charge density is often observed from disordered semiconductors, in which transport is limited by shallow traps.[34,35] For those materials, charge transport is

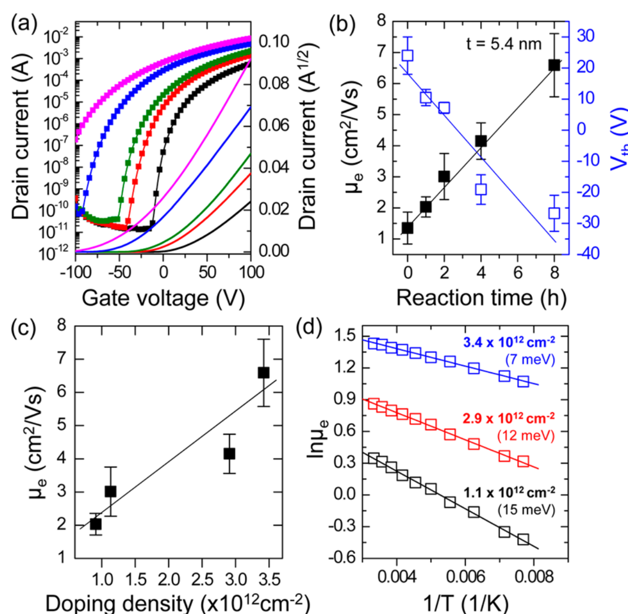

Figure 3. (a) Transfer characteristics (V_D = 60 V) of TFTs based on 5.4 nm thick ZnO film after the CTDL treatment for different periods of time (0, 1, 2, 4, and 8 h). (b) Electron mobilities and threshold voltages of ZnO TFTs extracted from (a). (c) Electron mobilities as a function of doping density by the CTDL. (d) Temperature-dependent electron mobility of pristine and CTDL-doped ZnO TFTs with various CTDL treatment times (0, 2, and 4 h).

accelerated, if more numbers of traps are filled by induced carriers.[36] To confirm whether this explanation is applicable to our system, we carried out temperature-dependent transport measurements (130−300 K) and extracted the activation energy (E_A) necessary for charge transport in ZnO films with different doping concentrations. Figure 3d displays the Arrhenius plot of the electron mobility for 5.4 nm ZnO films with three different charge tranfer doping concentrations (1.1 × 10^{12}, 2.9 × 10^{12}, and 3.4 × 10^{12} electrons/cm^2). E_A was reduced from 15 meV (pristine ZnO) to 7 meV (doped ZnO) upon increasing charge transfer doping, which is likely due to the reduced numbers of shallow traps. In addition, bias-stress stability measurement was performed by monitoring the I_D drop for the CTDL-doped ZnO TFTs over a period of time (t) under a constant V_G (100 V) and V_D (60 V). As shown in Figure S6 (Supporting Information), a less significant drop in I_D was observed for more doped ZnO films, which also suggests that influences of traps become suppressed with the charge transfer doping. Overall, the temperature-dependent transport measurements and the bias-stress measurements indicate that the origin of the improved mobility from the charge transfer doping is associated with filling of shallow traps upon doping.

We note that the estimated doping density of $\sim 10^{12}$ electrons/cm^2 is around 10% of the ballpark maximum doping concentration achievable from the APS charge transfer doping. The maximum value can be obtained from a relation $q = p/dA$, assuming that APS molecules are self-assembled in an ideal manner (uniform and monolayered). Here, q is the areal charge density induced in ZnO by the CTDL, p is the dipole moment defined when equal negative and positive charge densities are separated by a finite distance (d), and A is the lateral area per a single APS molecule (∼0.3 nm^2).[30,37] p and d of an APS molcule were estimated to be 3.19 D and 0.74 nm from a commercially available DFT calculation tool. These numbers

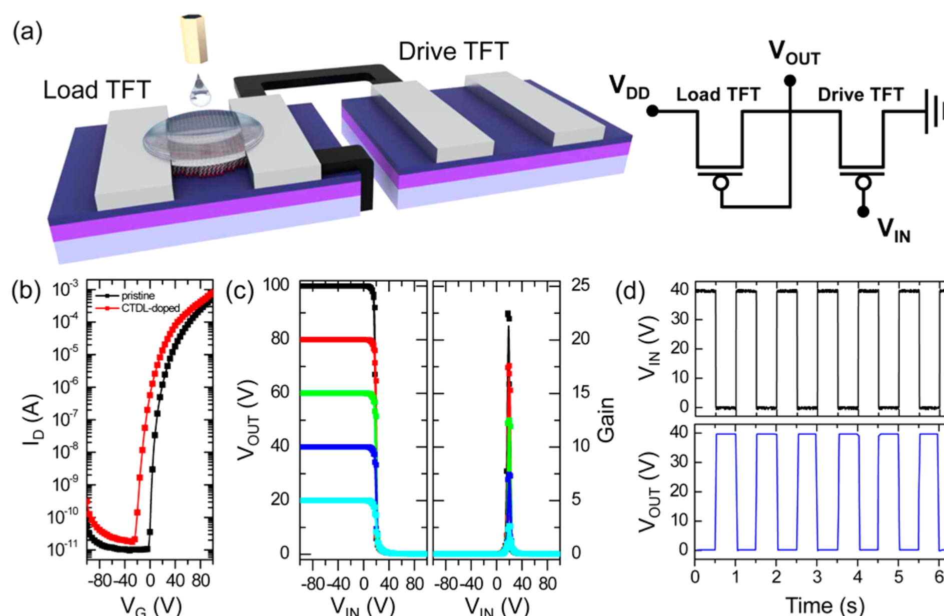

Figure 4. (a) Schematic and circuit diagram of a depletion load inverter based on an enhancement-mode drive TFT and a depletion-mode load TFT using pristine ZnO TFTs and CTDL-doped ZnO TFTs, respectively. (b) Transfer characteristics (V_D = 60 V) of ZnO TFTs based on 5.4 nm thick ZnO films before and after inkjet printing a single drop of CTDL solution. (c) The voltage transfer characteristics of the inverter under various V_{DD}'s (from 20 to 100 V; interval = 20 V) and their corresponding signal gain. (d) Output voltage response of the depletion load inverter at V_{DD} = 40 V when V_G is pulsed at 1 Hz.

yield $q = 3.0 \times 10^{13}$ carriers/cm^2, which is about an order of magintude larger than what we achieved. The discrepancy between the estimation and the experimental results is perhaps because our APS layers are not assembled in an ideal manner: atomic force microscopy (AFM) images reveal formation of globules from ZnO films that were applied to APS for longer time (Figure S3, Supporting Information). The results indicate that electron mobility of APS-treated ZnO films can be further enhanced if the CTDL is formed more uniformly.

The capability of simple threshold voltage control of the CTDL could be employed for unconventional logic circuit designing. For example, high-performance depletion load ZnO inverters were successfully demonstrated from simple solution processes. The depletion load inverter comprises an enhancement-mode drive transistor and a depletion-mode load transistor in series (Figure 4a). This combination allows the formation of an inverter logic circuit without varying the W/L ratio between respective transistors, which is beneficial for compact device integration. A pristine ZnO TFT and a CTDL-doped ZnO TFT were employed as the drive and the load, respectively. In fact, the possibility of introducing CTDL on top of the active layer offers practical advantages in fabricating logic circuits in a simpler manner over the methods utilizing a functional layer under the active layer. Namely, CTDL could be applied selectively onto a ZnO TFT designated as the load transistor using a simple inkjet printing method. Such a method also avoids wetting issues of the active layer that is likely to occur if the functional layer is to be applied under the active layer selectively.

Figure 4b displays the transfer characteristics of a pristine ZnO TFT and a doped ZnO TFT (thickness of ZnO = 5.4 nm) obtained by printing a single drop of CTDL solution onto the active layer. The V_{th} are 40.1 and 12.9 V, respectively. The difference in V_{th} yielded large separation of the current level between the two transistors, which is beneficial for forming a high-performance inverter. As shown in the circuit diagram in Figure 4a, the source electrode of the load transistor was connected to the gate electrode of the load transistor and drain electrode of the drive transistor. The working principles of these devices are described well in the previous literature.[38] The resulting inverters exhibited ideal voltage−transfer characteristics with negligible hysteresis, as shown in Figure 4c. As the supply voltage (V_{DD}) was increased from 20 to 100 V, the output voltage (V_{OUT}) remained comparable to the V_{DD} values at low input voltages (V_{IN}) and was 0 V at high V_{IN}. The signal inverter gain, defined as the absolute value of dV_{OUT}/dV_{IN}, is also provided in Figure 4c as a function of V_{DD}. A maximum gain value of 23 was obtained at V_{DD} = 100 V. Moreover, this CTDL doping method of ZnO could be applied to high-capacitance gate dielectrics, for example, a thinner SiO_2 layer, yielding low voltage operation of the devices, as shown in Figure S7 (Supporting Information). Figure 4d exhibits the dynamic response characteristics of the inverter output signal obtained under V_{DD} = 40 V. The output voltage of the inverter responded well to a square-wave input voltage signal.

4. CONCLUSIONS

In conclusion, we demonstrated a new doping method utilizing charge transfer doping based on APS to achieve high-performance ZnO transistors and inverters. The strong electron-donating characteristics of the amine group in APS molecules filled shallow electron traps residing in the ZnO films and thereby yielded a dramatic enhancement in the electron mobility. The optimized ZnO thickness and APS grafting density resulted in ZnO TFTs with excellent device characteristics; electron mobility as high as 4.2 cm^2/(V s) was achieved while exhibiting the on/off current ratio of more than 10^7. Furthermore, the facile threshold voltage control of this method allowed assembling high-performance depletion load ZnO inverters successfully via selective application of CTDL onto a ZnO film based on simple inkjet printing processes. We believe that the method presented herein can make significant

dx.doi.org/10.1021/am402919f | ACS Appl. Mater. Interfaces 2013, 5, 9765−9769

contributions to achieve next-generation high-performance TFTs for plastic electronics for flexible, printed, and transparent electronics.

■ ASSOCIATED CONTENT

Supporting Information

XPS spectra and AFM images of the pristine and CTDL-doped ZnO films, electrical characteristics of ZnO TFTs based on ZnO films with different thicknesses before and after the CTDL treatment, bias stability measurement of ZnO TFTs, electrical characteristics of the ZnO TFTs and inverters based on a 100 nm thick SiO_2, and summarized electrical parameters of ZnO TFTs are available. This material is available free of charge via the Internet at http://pubs.acs.org.

■ AUTHOR INFORMATION

Corresponding Authors

*E-mail: jylee7@skku.edu.
*E-mail: jhcho94@skku.edu.

Notes

The authors declare no competing financial interest.

■ ACKNOWLEDGMENTS

This research was done in the KANEKA/SKKU Incubation Center and financially supported by Kaneka Corp. in Japan, a grant (no. 2011-0031628) from the Center for Advanced Soft Electronics under the Global Frontier Research Program of the Ministry of Education, Science and Technology, and the Basic Research Program through the National Research Foundation of Korea (NRF) funded by the Ministry of Education, Science and Technology (NRF-2013R1A2A2A01015700 and 2009-0083540).

■ REFERENCES

(1) Kim, M. G.; Kanatzidis, M. G.; Facchetti, A.; Marks, T. J. *Nat. Mater.* **2011**, *10*, 382−388.
(2) Banger, K. K.; Yamashita, Y.; Mori, K.; Peterson, R. L.; Leedham, T.; Rickard, J.; Sirringhaus, H. *Nat. Mater.* **2011**, *10*, 45−50.
(3) Arias, A. C.; MacKenzie, J. D.; McCulloch, I.; Rivnay, J.; Salleo, A. *Chem. Rev.* **2010**, *110*, 3−24.
(4) Sun, Y. G.; Rogers, J. A. *Adv. Mater.* **2007**, *19*, 1897−1916.
(5) Yan, H.; Chen, Z. H.; Zheng, Y.; Newman, C.; Quinn, J. R.; Dotz, F.; Kastler, M.; Facchetti, A. *Nature* **2009**, *457*, 679−686.
(6) Choi, J.-H.; Kar, J. P.; Das, S. N.; Lee, T. I.; Khang, D.-Y.; Myoung, J.-M. *J. Mater. Chem.* **2011**, *21*, 2303−2309.
(7) Adamopoulos, G.; Bashir, A.; Wobkenberg, P. H.; Bradley, D. D. C.; Anthopoulos, T. D. *Appl. Phys. Lett.* **2009**, *95*, 133507.
(8) Bolink, H. J.; Coronado, E.; Orozco, J.; Sessolo, M. *Adv. Mater.* **2009**, *21*, 79−82.
(9) Ong, B. S.; Li, C.; Li, Y.; Wu, Y.; Loutfy, R. *J. Am. Chem. Soc.* **2007**, *129*, 2750−2751.
(10) Frenzel, H.; Lajn, A.; von Wenckstern, H.; Lorenz, M.; Schein, F.; Zhang, Z.; Grundmann, M. *Adv. Mater.* **2011**, *23*, 1425−1425.
(11) Sun, B.; Sirringhaus, H. *J. Am. Chem. Soc.* **2006**, *128*, 16231−16237.
(12) Hoffman, R. L.; Norris, B. J.; Wager, J. F. *Appl. Phys. Lett.* **2003**, *82*, 733−735.
(13) Song, K.; Noh, J.; Jun, T.; Jung, Y.; Kang, H.-Y.; Moon, J. *Adv. Mater.* **2010**, *22*, 4308−4312.
(14) Bong, H.; Lee, W. H.; Lee, D. Y.; Kim, B. J.; Cho, J. H.; Cho, K. *Appl. Phys. Lett.* **2010**, *96*, 192115.
(15) Park, S. Y.; Kim, B. J.; Kim, K.; Kang, M. S.; Lim, K.-H.; Lee, T. I.; Myoung, J. M.; Baik, H. K.; Cho, J. H.; Kim, Y. S. *Adv. Mater.* **2012**, *24*, 834−838.
(16) Liu, W.; Xiu, F.; Sun, K.; Xie, Y.-H.; Wang, K. L.; Wang, Y.; Zou, J.; Yang, Z.; Liu, J. *J. Am. Chem. Soc.* **2012**, *132*, 2498−2499.
(17) Chang, J.; Lin, Z.; Zhu, C.; Chi, C.; Zhang, J.; Wu, J. *ACS Appl. Mater. Interfaces* **2013**, *5*, 6687−6693.
(18) Kim, K.; Park, S.; Seon, J.-B.; Lim, K.-H.; Char, K.; Shin, K.; Kim, Y. S. *Adv. Funct. Mater.* **2011**, *21*, 3546−3553.
(19) Yamamoto, N.; Makino, H.; Osone, S.; Ujihara, A.; Ito, T.; Hokari, H.; Maruyama, T.; Yamamoto, T. *Thin Solid Films* **2012**, *520*, 4131−4138.
(20) Sun, Q.; Seo, S. *Org. Electron.* **2012**, *13*, 384−387.
(21) Jung, Y.; Yang, W.; Koo, C. Y.; Song, K.; Moon, J. *J. Mater. Chem.* **2012**, *22*, 5390−5397.
(22) Gabas, M.; Landa-Canovas, A.; Costa-Kramer, J. L.; Agullo-Rueda, F.; Gonzalez-Elipe, A. R.; Diaz-Carrasco, P.; Hernandez-Moro, J.; Lorite, I.; Herrero, P.; Castillero, P.; Barranco, A.; Ramos-Barrado, J. R. *J. Appl. Phys.* **2013**, *113*, 163709.
(23) Nomura, K.; Ohta, H.; Takagi, A.; Kamiya, T.; Hirano, M.; Hosono, H. *Nature* **2004**, *432*, 488−492.
(24) Kim, Y. H.; Heo, J. S.; Kim, T. H.; Park, S.; Yoon, M. H.; Kim, J.; Oh, M. S.; Yi, G. R.; Noh, Y. Y.; Park, S. K. *Nature* **2012**, *489*, 128−132.
(25) Zan, H.-W.; Tsai, W.-W.; Chen, C.-H.; Tsai, C.-C. *Adv. Mater.* **2011**, *23*, 4237−4242.
(26) Hoffmann, R. C.; Kaloumenos, M.; Heinschke, S.; Erdem, E.; Jakes, P.; Eichel, R.-A.; Schneider, J. J. *J. Mater. Chem. C* **2013**, *1*, 2577−2584.
(27) Kamiya, T.; Nomura, K.; Hosono, H. *Sci. Technol. Adv. Mater.* **2010**, *11*, 044305.
(28) Aksu, Y.; Driess, M. *Angew. Chem., Int. Ed.* **2009**, *48*, 7778−7782.
(29) Demchenko, D. O.; Earles, B.; Liu, H. Y.; Avrutin, V.; Izyumskaya, N.; Ozgur, U.; Morkoc, H. *Phys. Rev. B* **2011**, *84*, 075201.
(30) Heiney, P. A.; Gruneberg, K.; Fang, J. Y.; Dulcey, C.; Shashidhar, R. *Langmuir* **2000**, *16*, 2651−2657.
(31) Calhoun, M. F.; Sanchez, J.; Olaya, D.; Gershenson, M. E.; Podzorov, V. *Nat. Mater.* **2008**, *7*, 84−89.
(32) Lee, J.; Kim, K.; Kim, J. H.; Im, S.; Jung, D. Y. *Appl. Phys. Lett.* **2003**, *82*, 4169−4171.
(33) Natsume, Y.; Sakata, H. *Thin Solid Films* **2000**, *372*, 30−36.
(34) Park, C. H.; Zhang, S. B.; Wei, S. H. *Phys. Rev. B* **2002**, *66*, 073202.
(35) Orlinskii, S. B.; Schmidt, J.; Baranov, P. G.; Hofmann, D. M.; Donega, C. D.; Meijerink, A. *Phys. Rev. Lett.* **2004**, *92*, 047603.
(36) Kline, R. J.; McGehee, M. D. *Polym. Rev.* **2006**, *46*, 27−45.
(37) Ellison, D. J.; Lee, B.; Podzorov, V.; Frisbie, C. D. *Adv. Mater.* **2011**, *23*, 502−507.
(38) Han, S. T.; Zhou, Y.; Xu, Z. X.; Roy, V. A. L. *Appl. Phys. Lett.* **2012**, *101*, 033306.